

GEOID COMPUTATION IN THE MEDITERRANEAN AREA

R. Barzaghi, M. Brovelli, F. Sansó

DIAR - Politecnico di Milano

P.za Leonardo da Vinci 32, 20133 Milano, ITALY

C. C. Tscherning

Geophysical Institute - University of Copenhagen

Haraldsgade 6, DK-2200 Copenhagen, DENMARK

1. Introduction

This paper deals with the computation of a gravimetric geoid on a large area covering the Western part of the Mediterranean Sea. This is done in the framework of the Geomed project which aims at evaluating a high precision geoid in the whole Mediterranean area. What we have done can be considered a first experiment suitable to define the numerical and theoretical methods to be applied on the global area. The techniques we used to estimate the geoid undulation from gravity data are Stokes/FFT formula (Sideris 1987, Forsberg and Solheim, 1988) and Fast Collocation (Bottoni and Barzaghi, 1991). This allowed us to obtain the solution in one step only, overcoming the patching of local solutions computed on a partition of the area under investigation. The first important comparison we derived is the one on the two different methods we applied on the same gravity data base; to the knowledge of the author this is the first time that an FFT derived geoid is compared with a collocation solution computed in one step on such a large area. A second check on the estimated geoid has been obtained by comparison with the adjusted altimetry data (both from GEOSAT and SEASAT satellites). A byproduct of this is an estimate of the Sea Surface Topography (SST) which gave us a first insight on the water circulation pattern in the western part of the Mediterranean Sea.

2. Some remarks on geoid estimation

The method we used to estimate the geoid is the remove-restore technique (Forsberg, 1985, Tscherning, 1985, Arabelos and Tscherning, 1988). As it is well known, while using such a procedure one splits the geoid computation in the following steps:

- remove the effect of a global geopotential model from the data;
- remove the Residual Terrain Effect (RTE) from the data, i.e. the effect implied by the masses between the topography and a proper, smooth reference topography (usually obtained from the detailed digital terrain model applying a proper low-pass filter);
- estimate, using the reduced data, the residual geoid using one method or another (collocation, Stokes and so on);
- restore the RTE in terms of geoid undulation, adding this effect to the residual geoid;
- restore the geoid undulation implied by the global geopotential model.

This method, as it is evident, performs a frequency analysis of the data, removing the low frequency part (the geopotential model) and the high frequency component (RTE). Removing the global geopotential model localizes the data so that only the correlations between points in the local area are significant; the subtraction of the RTE regularizes strongly the data decoupling these from the main topographic features and their high frequency signal. So, the reduced signal should have suitable statistical properties (nearly zero mean and small variance) and should not contain any relevant trend; consequently, collocation (or else) gives an optimal estimate of the residual geoid. Although this procedure is nowadays commonly used, there are still some critical points in its practical application. As pointed out before, the global geopotential models should remove the low frequency components from the data; unfortunately, in some regions, these geopotential models contain biases and do not represent properly the gravity field. This is the case of the southern and the eastern Europe areas because of the lack of data in the eastern Europe nations and in Africa.

Furthermore, the methods used to compute the coefficients of the spherical harmonic series of the Earth gravitational potential lead to biased estimates (Albertella and others, 1981). Thus, the subtraction of the global geopotential model can introduce significant distortions, that is non zero

mean residuals and/or no suitable modelling of the trend present in the residual data.

The second step of the remove-restore method can give rise to problems too. There are no precise rules to define the smooth reference terrain model to compute the RTE. Since it is supposed that the global geopotential model accounts also for the low-frequency part of the topographic signal, one is confronted with the problem of defining the proper smoothed version of the topography, which should be the one implied by the geopotential model. However, as noticed before, the geopotential models are in some cases unreliable and sometimes poorly correlated with the main topographic features. If we consider them from a local point of view, phase shifts can occur between observed and model implied values, causing problems both in trend removal and RTE computation.

The definition of the reference surface for RTE computation is crucial; if we define it properly we can reduce the data in a coherent way, producing the expected regularization of the data. In practical applications different rules of thumb are adopted but no theoretical procedure has been devised. Hence, we cannot be sure that the second step of the remove procedure is correctly done because we cannot state that the reference smooth topography matches with the selected geopotential model (see fig. 1)¹.

This can give problems when areas of about 2° of size are considered; if the topography in the area is rough and the surface implied by the model differs from the one used for the RTE computation, a significant medium frequency trend can remain in the residual values. This trend is obviously related to the effect of the masses between the two reference surfaces mentioned before (see fig 1.) and can compromise the next step of the geoid estimation (if, for instance, we use collocation on the residuals and a trend is still present, we can have distortions in the geoid estimate). In the numerical tests we did in the Mediterranean Sea, we selected a quite large area ($35^\circ \leq \phi \leq 45^\circ$; $-5^\circ \leq \lambda \leq 10^\circ$); thus, the problems due to the removal of a geopotential model effect and to an improper RTE reduction, in the sense specified before, should not introduce a so relevant trend that collocation cannot handle. Hence, we simply averaged the higher resolution DTM to obtain the smooth reference

¹ A possible correct procedure could be to vary the reference surface until the residual signal, i.e. data minus the model and the RTE contribution, decorrelates with the geopotential model

surface used for the RTE computation.

The results we got, seem to confirm that, in our case, the problems related to the model and to the RTE computation are not critical.

The final remark refers to the gridding of the data. Since we applied Stokes/FFT and the Fast Collocation methods, we needed gridded homogeneous data. We applied the gridding procedure to the smoothed gravity data, that is to

$$\Delta g_r = \Delta g_0 - \Delta g_M - \Delta g_{RTE} \quad (2.1)$$

to minimize gridding errors. It is in fact evident that Δg_r data can be interpolated in a more accurate way than Δg_0 because of their optimal spectral properties (i.e. only medium wave components).

3. The gravimetric geoid computation

In the Western Mediterranean area we have a good data coverage. In the selected window

$$\begin{aligned} 35^\circ &\leq \phi \leq 45^\circ \\ -5^\circ &\leq \lambda \leq 10^\circ \end{aligned} \quad (3.1)$$

there are 7944 marine gravity data (placed on a regular grid of 5'x5') and 28837 gravity data on land.

The marine gravity data were supplied by D. Arabelos (1988) while the terrestrial gravity data comes from the BGI or from the data base of the research group involved in the GEMED project; terrestrial gravity data are

subdivided according to tab. 1.

Nation	N. of data
ALGERIA	1738
FRANCE	5196
ITALY	1010
MAROCCO	433
SPAIN	20209
TUNISIA	51

Tab. 1. - Available gravity data on land

The statistical properties of these data are summarized by the figures

$$E(\Delta g) = 11.12 \text{ mgal}$$

$$\sigma(\Delta g) = 31.51 \text{ mgal}$$

and the contour line plot of these data is represented in fig. 2. As one can see, there are sharp variations in the terrestrial gravity mainly related to the topography of the area which is quite rough in the north-west corner (Pyrenees Mountain chain) and close to the southern part (Altante Mountain chain). On the contrary, the sea floor is quite smooth (fig. 4) and this reflects in the feature of the marine gravity data. Because of this heterogeneity, the remove-restore technique becomes an inappropriate method to get a good geoid estimate. Furthermore, the problems related to the remove steps pointed out previously should not be relevant as the selected area is quite large; hence the computation can be carried out without any further refinement of the remove-restore procedure.

We firstly subtracted the gravity effect of a global geopotential model; the one we used for the computation is the OSU91A by R.H. Rapp (1991) plotted in fig. 3.

To model and remove the RTE we used the TUG87 terrain model (Weiser, 1987) which gives the topography/bathymetry of the Earth on a regular grid of 5'x5'. The smooth reference topography was computed from the TUG87 with a moving average of 15'x15'; TUG87 and its smoothed version in the selected area are plotted in fig.4 and fig.5.

To compute the RTE we used the TC program by R. Forsberg which gives the gravity terrain component using the rigorous formula of the gravity effect on a parallelepiped; this correction was obtained considering all the parallelepipeda with centers contained in a circle centered on the computation point with radius 100 km.

At the end of the remove procedure, we had the residual gravity of fig. 6. As expected, no relevant trend are present, the main topographic irregularities disappeared, the dominant frequency pattern of the residual gravity is a medium one and the signal has been smoothed significantly. This can be also deduced from table 2 where the statistics of the remove procedure are listed (note that the number of data decreases because, during the processing procedure, outliers have been rejected).

	N. of data	Average (mgal)	St. dev. (mgal)
Δg	36581	11.12	31.51
$\Delta g - \Delta g_{OSU91A}$	36570	-3.92	25.88
$\Delta g_r = \Delta g - \Delta g_{OSU91A} - \Delta g_{RTE}$	36570	0.35	16.97

Tab. 2. - Remove statistics

The gridding procedure has been applied on Δg_r using the GEORGR program developed by R. Forsberg, performing a spline interpolation and producing a geographical grid with grid side of 5'. Thus, in the selected area, 17557 gridded gravity data Δg_r^G with the following statistical parameters are obtained:

$$E(\Delta g_r^G) = 1.22 \text{ mgal}$$

$$\sigma(\Delta g_r^G) = 14.50 \text{ mgal}$$

Note that the gridding procedure leads to a gravity data set statistically close to the original Δg_r data set; this suggests that the choice of gridding the smooth Δg_r values. To start with the collocation procedure to get the residual geoid, the empirical covariance function of Δg_r which is plotted in fig. 1. As one can notice, the correlation length is nearly 15' confirming that the empirical covariance function doesn't contain long wavelength trends. The selected best fit model obtained using the COVFIT program by Knudsen (1987), was of the form:

$$C(P,Q) = C(\psi_{PQ}) = \sum_{i=1}^m \sigma_1^e \left[\frac{R^2}{r_P r_Q} \right]^{n+2} P_n(\cos \psi_{PQ}) + \sum_{i=m+1}^{\infty} \sigma_1 \left[\frac{R^2}{r_P r_Q} \right]^{n+2} P_n(\cos \psi_{PQ})$$

where σ_1^e are the error-degree variances used up to $m=120$ and

$$\sigma_1 = \frac{(i-1)^2}{R^2} A \frac{(1-i)}{(i-1)(i-2)(i+24)}$$

R = mean Earth radius

The selected depth of the Bjerhammar sphere was $R_B - R = -2393.725$ m and the noise variance level was fixed to 4 mgal^2 .

The output of Stokes/FFT and Fast Collocation are practically the same (see fig. 8 and fig. 9). This good fitting between the two estimates is confirmed by the correlation coefficient $\rho = 0.98$; hence, the comparison between the two procedures leads to a very encouraging result. The main difference between the two solutions is a bias; the collocation solution is 45 cm higher than the Stokes/FFT derived undulation (which has zero average - see tab. 2). This discrepancy in the mean can be explained taking into account that in the Stokes/FFT procedure we removed the average of the gravity data ($E(\Delta g_r) = 1.22 \text{ mgal}$) and that we didn't do the same for the collocation procedure. In the Stokes/FFT method, to damp the high frequency part of the spectrum of the data induced by the non zero average which can cause instabilities in the computing procedure. On the contrary, as this is not strictly necessary, we didn't remove the average in the collocation procedure. In trying, in this way, to overcome the "restore of the mean problem". This is another critical point in the whole estimation procedure; if we remove the mean from the gravity data, we cannot restore it in term of geoid undulation since, as it is well known, the potential implied by a constant gravity value tends to infinity in the planar approximation. So, rigorously speaking we can only compute relative geoid undulation since, by differentiating, we remove a common undefined bias. Furthermore, we stress that this problem becomes crucial when estimating a regional geoid by patching local solutions. If the local gravity data have different mean values, the local estimates will differ by uneven local constants which will not be restored properly exactly through this mechanism that patching biased local solutions will result in a medium wavelength distortion of the global geoid, as revealed by comparisons with GPS/levelling geoid.

In our case, since we computed directly the solution on the whole and we overcame the patching problem and, taking into account in the further steps the restore procedure the collocation estimate of N_r , we disregarded the "restore of the mean problem" discussed before; we simply let collocation compensate for the small non zero mean of Δg_r^G . This in fact is likely to happen when, in front of a grid spacing of $5'$, we have a process with a correlation length as it is in this case. Since the method is stable and the residual gravity data average is nearly zero, we can hopefully assume

relevant distortions are present in the estimated residual geoid; however, be cautious, we can say that we estimated, also in this case, a geoid.

The restore statistics are summarized in table 3 while the plots of RTE geoid, and of $N_M(OSU91A)$, the geopotential model implied geoid, $\hat{N}_r(FC)$, are represented in fig. 10 and fig. 11; the estimated geoid is in fig. 12.

	N. of data	Average (m)	St. d (m)
$\hat{N}_r(FFT)$	17557	0.00	0.66
$\hat{N}_r(FC)$	17557	0.45	0.67
$\hat{N}_r(FC) + N_{RTM}$	17557	0.54	0.67
$\hat{N} = \hat{N}_r(FC) + N_{RTM} + N_{OSU91A}$	17557	47.99	3.40

Tab. 3. - Restore statistics

4. The comparison between the gravimetric geoid and the adjusted altimetric data; Sea Surface Topography estimation.

The altimetric observations give the height of the satellite over the sea surface, measuring the travel time of a radar pulse. Assuming to know the satellite coordinates in a geocentric reference frame, one can compute the height H_{alt} of the sea surface over the mean earth ellipsoid. By definition, this quantity can be splitted up in two components, i.e. the geoid N and the Sea Surface Topography, ζ .

$$H_{alt} = N + \zeta$$

(4)

where ζ is the sum of two terms, the stationary ζ^0 and the time varying SST. Hence, in principle, one can estimate ζ using H_{alt} and an estimate of N . This very simplified scheme to compute ζ doesn't take into account the model errors of the altimetric measurement.

The main problem is related to the position of the satellite which is known with a certain degree of error due, to approximations in the estimation of the satellite orbit. As it is evident, the radial orbit error is critical when dealing with altimetric observation. This error however becomes visible in cross-over discrepancies, i.e. differences of heights between crossing tracks (southgoing and northgoing tracks); to compensate for radial orbit error, a cross-over adjustment procedure is adopted (Rowland, 1981).

For a local area, as the one we are dealing with, the radial orbit error is modelled using a straight line; the cross-over adjustment allows to estimate track by track bias and tilt, imposing the cross-over consistency condition. The rank deficiency related to this least squares problem (Schrama 1990, Barzaghi and others, 1992) can be removed, for instance, combining cross-over equations and fit equations of the along track observations to a model geoid (e.g. N_{OSUSIA}). At the end of the adjustment procedure, we have the \hat{H}_{alt} values which are suited to estimate ζ by comparison with \hat{N} . One point that must be stressed is that the radial orbit error estimate and removal produce a distortion in the estimate of ζ . The components of ζ having the same shape of the radial orbit error are modelled at the same time in the bias and tilt analysis. Hence, this component will be removed in \hat{H}_{alt} and in the derived quantity.

Following the procedure previously described, we adjusted the altimetric observations we had in the area, consisting of 3971 SEASAT values (arranged in 56 tracks, giving 254 cross-overs) and of 11062 GEOSAT values (arranged in 201 tracks, giving 1956 cross-overs).

The cross-over condition was combined to the fit equation of each track with the OSUSIA model geoid; separate adjustments were firstly performed on SEASAT and GEOSAT data. The statistics of the cross-over discrepancies

$$v_{ij} = H_{alt}^i - H_{alt}^j$$

and of the discrepancies with the model

$$\Delta_i = H_{alt}^i - N_{OSUSIA}^i$$

both for SEASAT and GEOSAT, before and after the adjustment procedure compared in table 4.

		v^0	Δ^0	\hat{v}	$\hat{\Delta}$
S E A S A T	E (m)	-0.01	1.24	0.00	0.00
	σ (m)	0.20	0.52	0.06	0.39
G E O S A T	E (m)	-0.82	-0.07	0.00	0.00
	σ (m)	0.30	0.62	0.04	0.31

Δ^0, v^0 = unadjusted values $\hat{\Delta}, \hat{v}$ = adjusted values

Tab. 4. - Cross-over adjustment results

The statistics of table 4 prove that rough GEOSAT data fit N_{OSUSIA} better than rough SEASAT data. The converse is true for the cross-over consistency of rough GEOSAT observations which is poorer than the one derived from SEASAT observations. These features are simple consequences of the different

preprocessing applied to the two altimetric data sets.

The SEASAT values we have were locally adjusted, for biases only, on the Mediterranean Sea (Cruz and Rapp, 1982) while GEOSAT data were globally adjusted (Denker and Rapp, 1990).

Since, the processed values are quite homogeneous, we decided to merge the altimetric observations from the two satellite in a global adjustment (148 values with 3704 cross-overs). The statistics related to the global set data are the following

$$\begin{aligned} E(\hat{v}) &= 0.00 \text{ m} & \sigma(\hat{v}) &= 0.05 \text{ m} \\ E(\hat{\Delta}) &= 0.02 \text{ m} & \sigma(\hat{\Delta}) &= 0.36 \text{ m} \end{aligned} \quad (4.)$$

and the corresponding $\hat{\Delta}$ are plotted in fig. 13.

To obtain the estimate of $\hat{\zeta}$, we interpolated the gridded $\Delta\hat{N} = \hat{N}_{\text{collo}} + \hat{N}_{\text{RTM}}$ values along the satellite tracks (note that the same model N_{OSU1A} was omitted here as in the $\hat{\Delta}$ values from altimetry) obtaining

$$E(\Delta\hat{N}) = 0.61 \text{ m} \quad \sigma(\Delta\hat{N}) = 0.42 \text{ m} \quad (4.)$$

The estimate of the SST

$$\hat{\zeta} = \hat{\Delta} - \Delta\hat{N} \quad (4.7)$$

is shown in fig. 14; the mean and the standard deviation of the $\hat{\zeta}$ are

$$E(\hat{\zeta}) = -0.59 \text{ m} \quad \sigma(\hat{\zeta}) = 0.32 \text{ m} \quad (4.8)$$

The main features of the SST are a quite picked minimum south-east of the Balearic Islands and a global trend placed nearly along the $\phi = 38^{\circ}$ parallel.

5. Conclusions

The comparison between Stokes/FFT and Fast Collocation solutions gave a result so that one of the aims of the present paper has been reached. Furthermore, the whole remove-restore technique has been critically reviewed in view of its application to the geoid estimation in the whole Mediterranean area. Although some problems are still unsolved from the theoretical standpoint, this procedure led to a proper geoid estimate as one can see in the comparison with altimetry.

The geoid we computed is by no means a high precision geoid. A more detailed validation of data must be carried out and a more detailed DTM should be used in the RTE computation. In fact, it is evident that the 5' x 5' TUG87 model is too poor to account for the high frequency pattern of the geoid. Another crucial point is the data acquisition; large areas of the Mediterranean region have no sufficient data coverage. So, to attain the goal of the GEOMED project, we shall have to fill in data gaps and acquire a more detailed DTM.

Nevertheless, this first geoid estimate proved the feasibility of this method and, as a first by-product, an estimate of the SST has been derived. Future more accurate estimates of the geoid and of the SST will be possible when compared to altimetry data of the ERS1 satellite.

References

- A. Albertella, F. Migliaccio, F. Sansó (1991). The aliasing effect and the coefficients estimation. Determination of the geoid, present and future. Symposium N^o 106, Milan, Italy, 1990, Springer-Verlag.
- D. Arabelos, C.C. Tscherning (1988). Gravity field mapping from satellite altimetry, sea-gravimetry and bathymetry in the Eastern Mediterranean. Geophysical Journal, 92.

- R. Barzaghi, M. Brovelli, P. Knudsen (1992). Different cross-over methods applied to altimeter data in the Mediterranean area. Accepted publication on Bollettino di Geofisica Teorica ed Applicata, Trieste, Italy.
- G. Bottoni, R. Barzaghi (1991). Fast Collocation. Determination of the geoid present and future. Symposium N° 106, Milan, Italy, 1990, Springer-Verlag.
- J. Y. Cruz, R. H. Rapp (1982). Sea surface heights in the Mediterranean area from Seasat altimeter data. Bollettino di Geofisica Teorica ed Applicata, vol. XXIV, n. 95, Trieste, Italy.
- H. Denker, R. H. Rapp (1990). Geodetic and Oceanographic results from the analysis of one year of Geosat data. Journal of geophysical Research, vol. 95, n. C8.
- R. Forsberg (1985). Gravity field terrain effect computation by FFT. Bulletin of Geodesique, 59, 4.
- R. Forsberg, D. Solheim (1988). Performance of FFT methods in local gravity field modelling. Chapman Conference on the Progress in the Determination of the Earth gravity field. Florida.
- P. Knudsen (1987). Estimation and modelling of local empirical covariance function using gravity and satellite altimeter data. Bulletin of Geodesique, 61, 2.
- R. H. Rapp, Y. M. Wang, N. Pavlis (1991). Geoid undulation differences between geopotential models. Presented to the XVI General Assembly of the IAGLR, EGS, Wiesbaden.
- D. Rowland (1981). The adjustment of Seasat altimeter data on a global basis for geoid and sea surface height determination. OSU Report 325, Columbus, Ohio.

- E. J. O. Schrama (1989). The role of orbit errors in preprocessing satellite altimeter data. Netherlands Geodetic Commission, n. 33, The Netherlands.
- M. Sideris (1987). Spectral Methods for the numerical solution of Molodensky's Problem. UCSE report, Calgary.
- C. C. Tscherning (1985). Local approximation of gravity potential by least-square collocation. K. P. Schwarz (Ed.): Proc. Int. Summer School on Local Gravity Field Approximation, Beijing, China, 1984, University of Calgary, Calgary, Canada.
- M. Weiser (1987). Das Globale Digitale Höhenmodell TUG87. Interner Bericht der Abteilung für Mathematische und Datenverarbeitende Geodäsie, Technische Universität, Graz.

Index of illustrations

- Fig. 1. - Improper reference surface in RTE computation
- Fig. 2. - Gravity anomalies in the Western Mediterranean area (mgal)
- Fig. 3. - Gravity anomalies implied by the geopotential model OSU91A (mgal)
- Fig. 4. - The TUG87 terrain model (m)
- Fig. 5. - The smoothed TUG87 terrain model (m)
- Fig. 6. - Residual gravity data Δg_r (mgal)
- Fig. 7. - The empirical covariance function of Δg_r
- Fig. 8. - Stokes/FFT residual geoid (m)

Fig. 9. - Fast Collocation residual geoid (m)

Fig. 10. - RTE geoid (m)

Fig. 11. - Geoid undulation implied by the geopotential model OSU91A (m)

Fig. 12. - The estimated gravimetric geoid (m)

Fig. 13. - Adjusted altimetry (GEOSAT and SEASAT data) minus OSU91A model
geoid (m)

Fig. 14. - Sea Surface Topography (m)

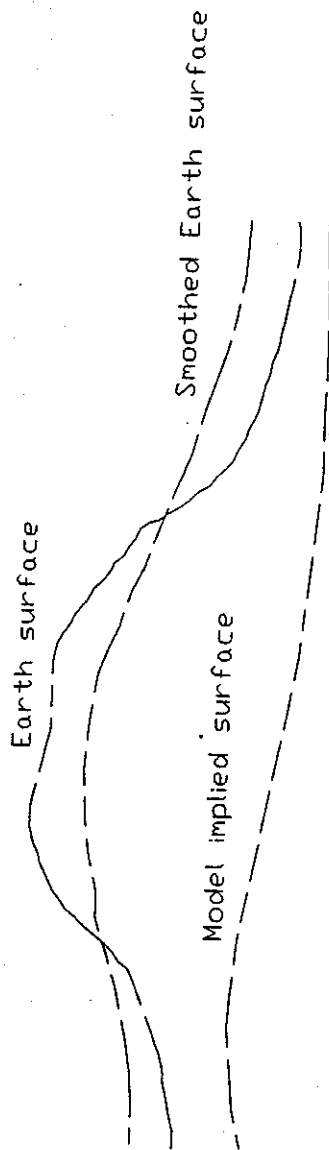
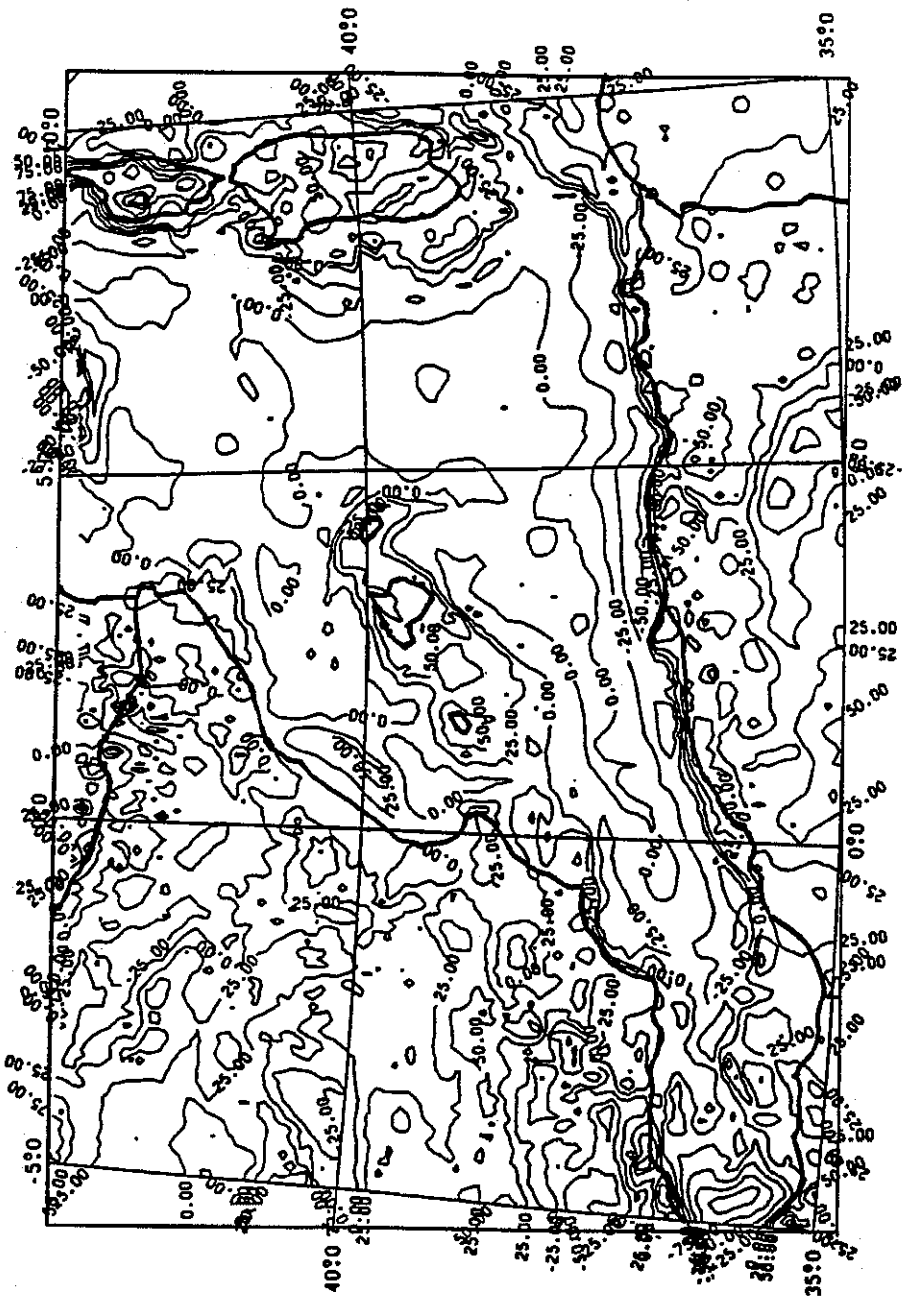
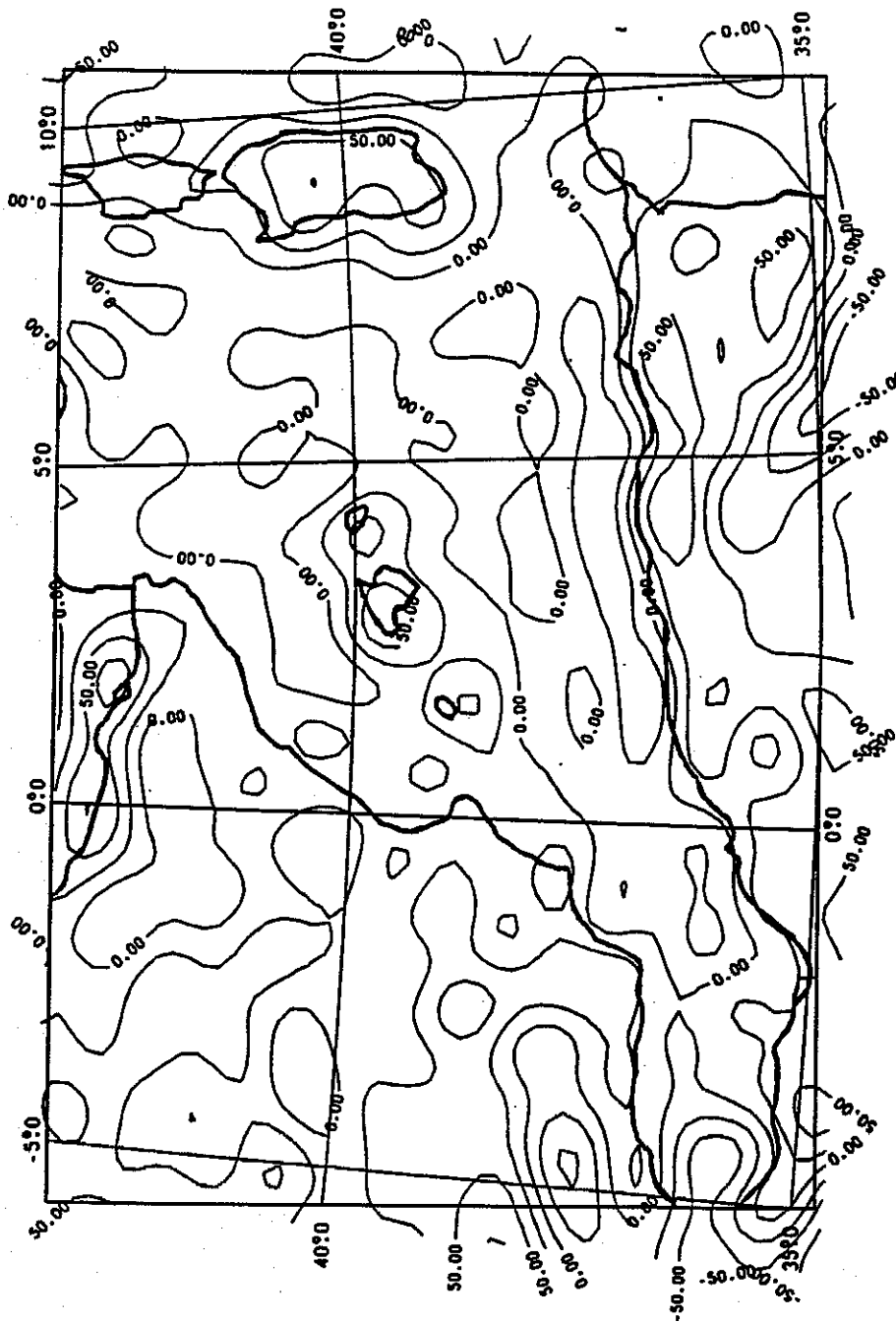
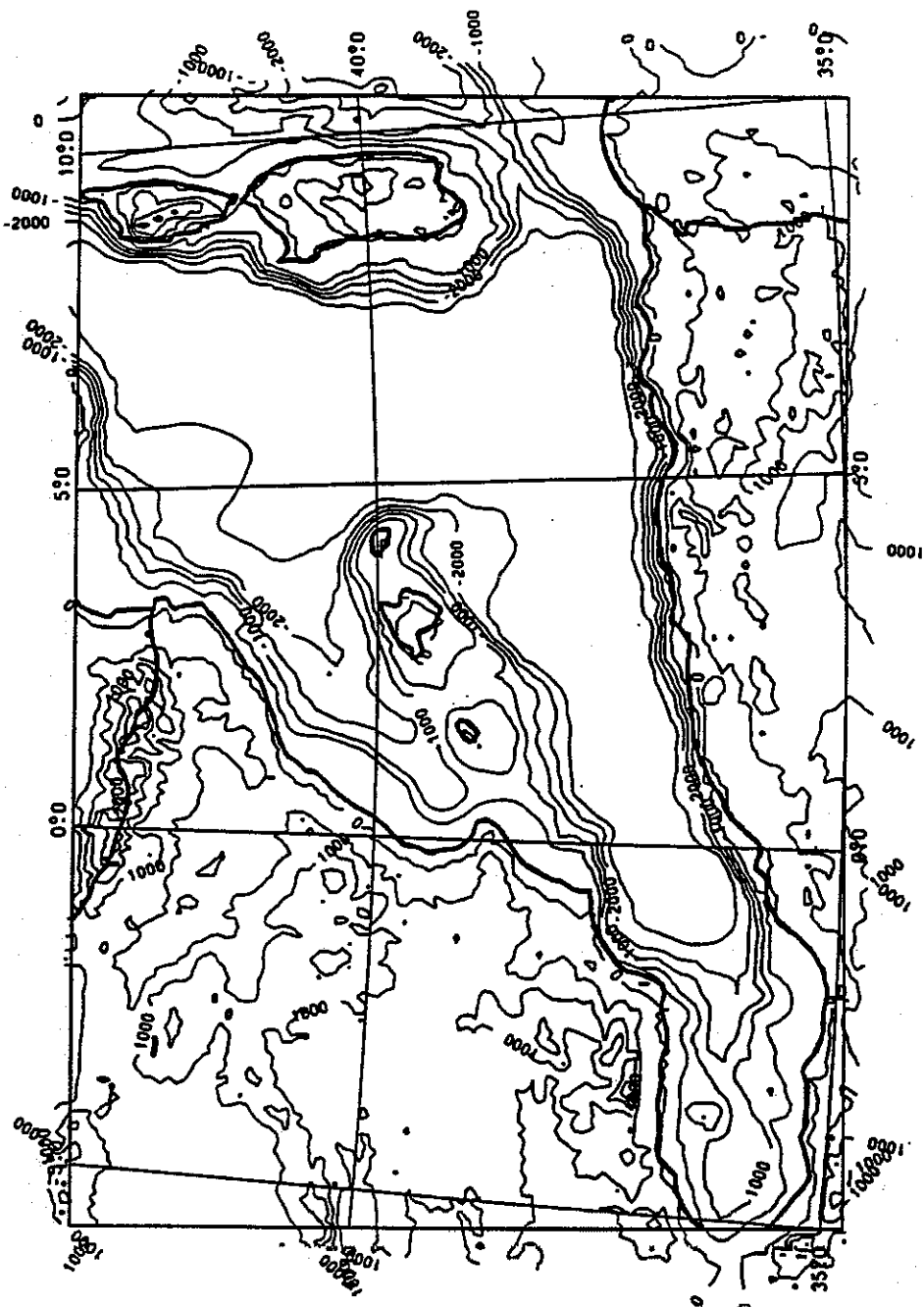
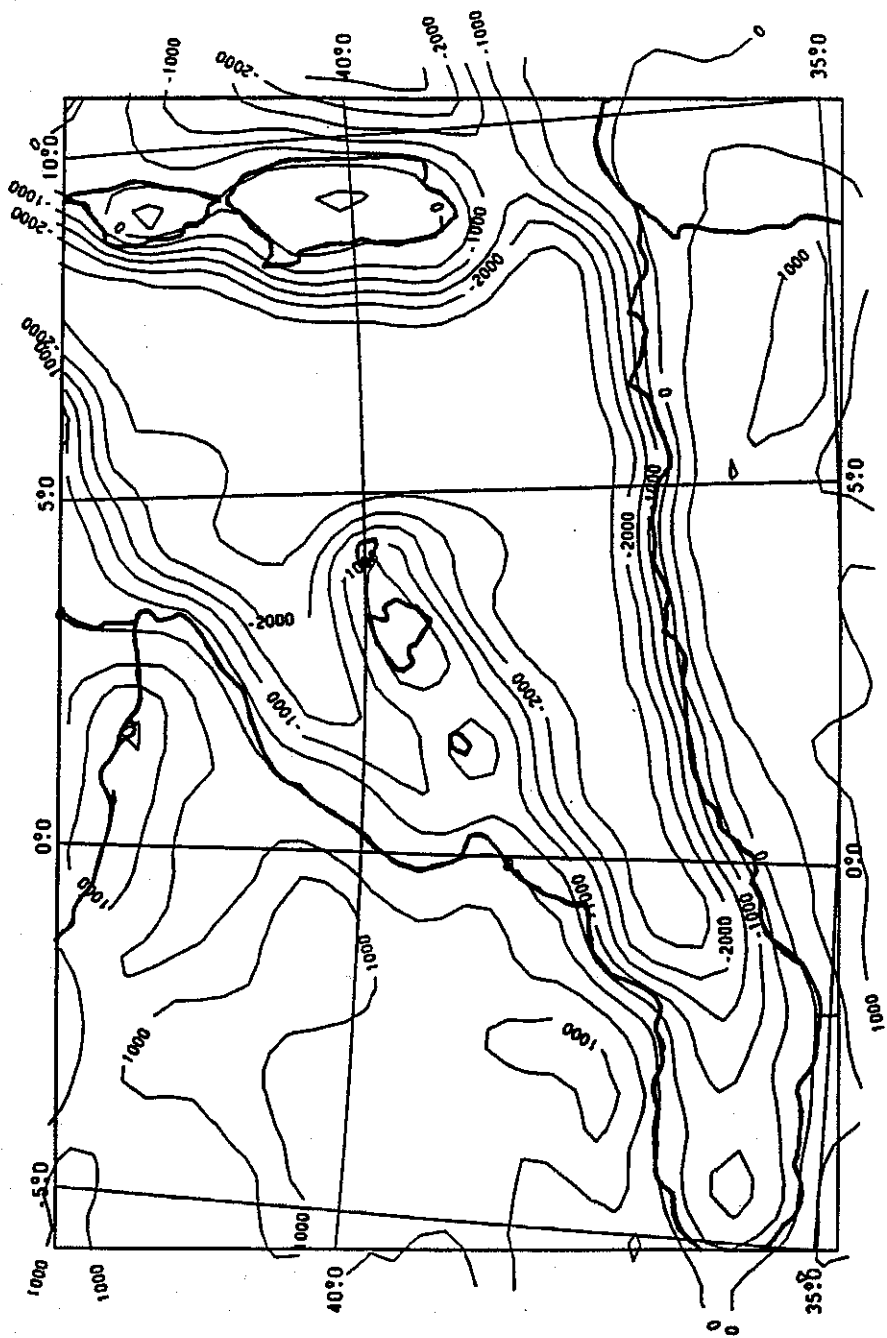


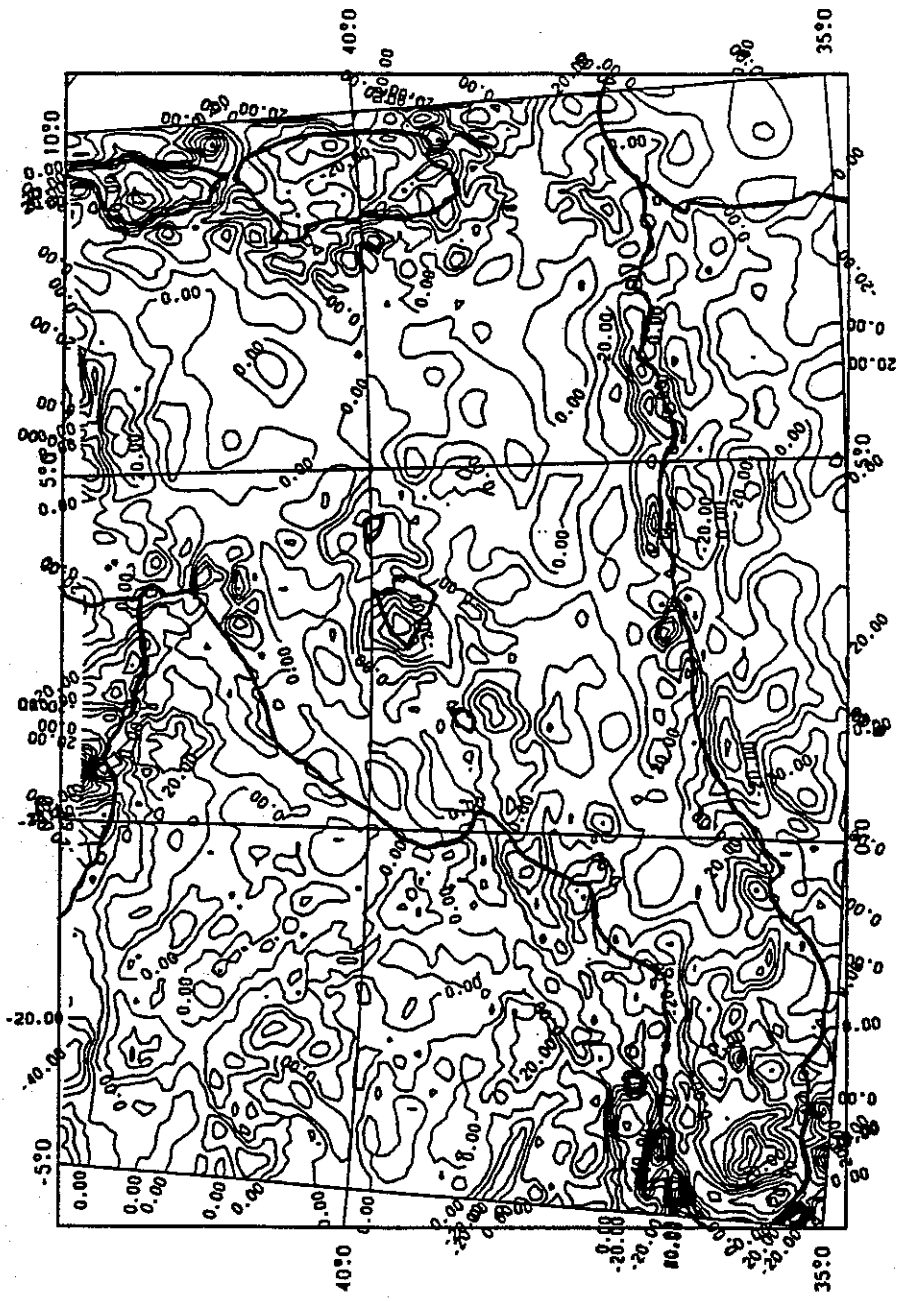
Fig. 1. - Improper reference surface in RTE computation

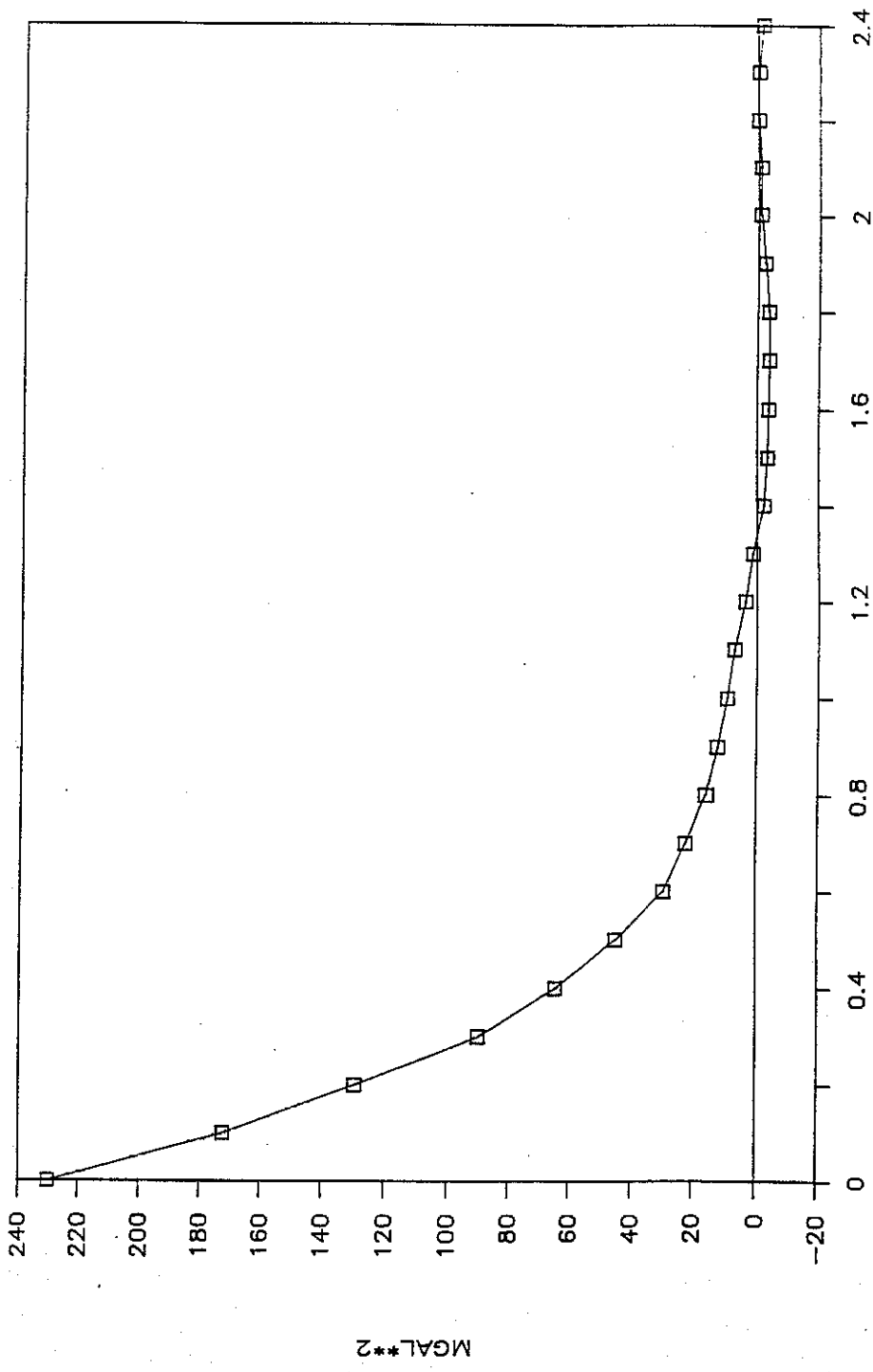












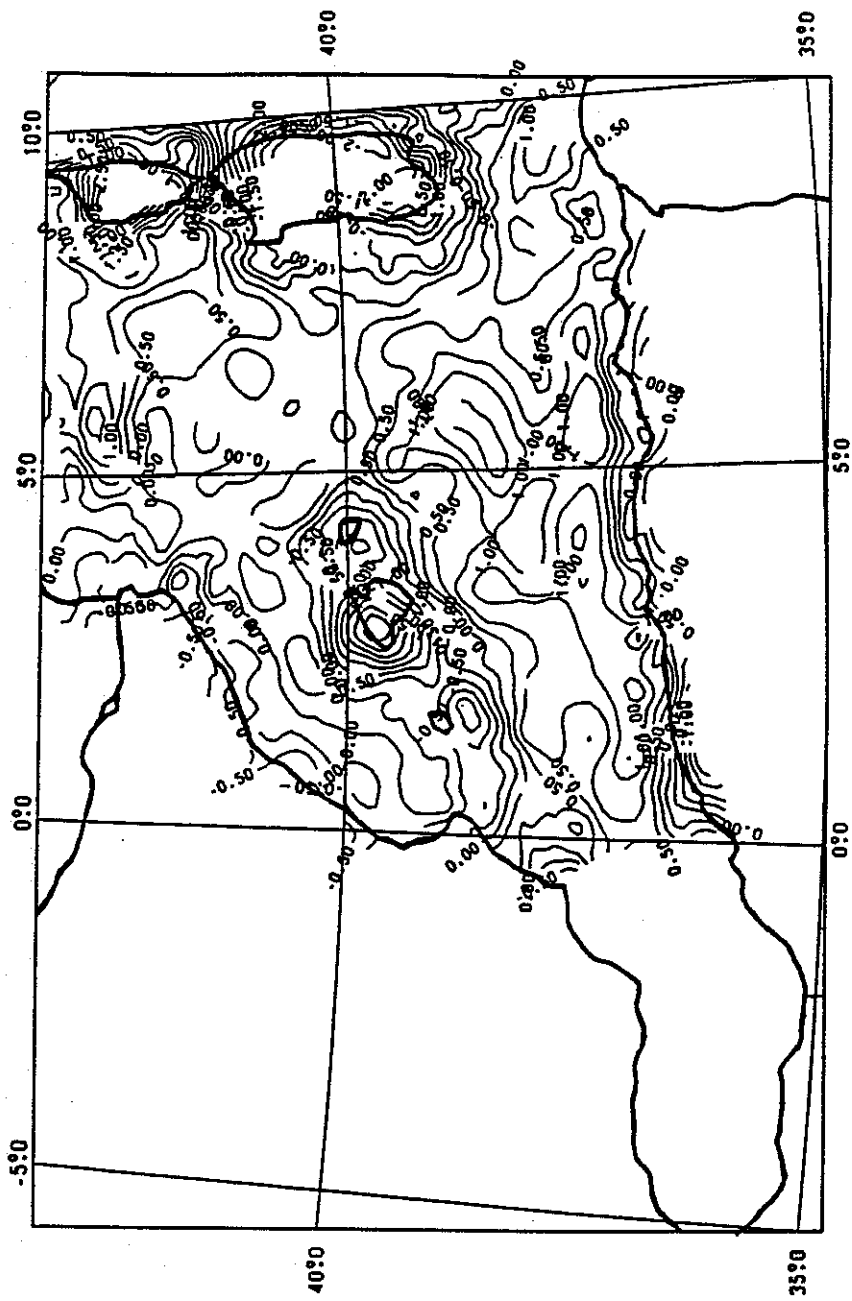
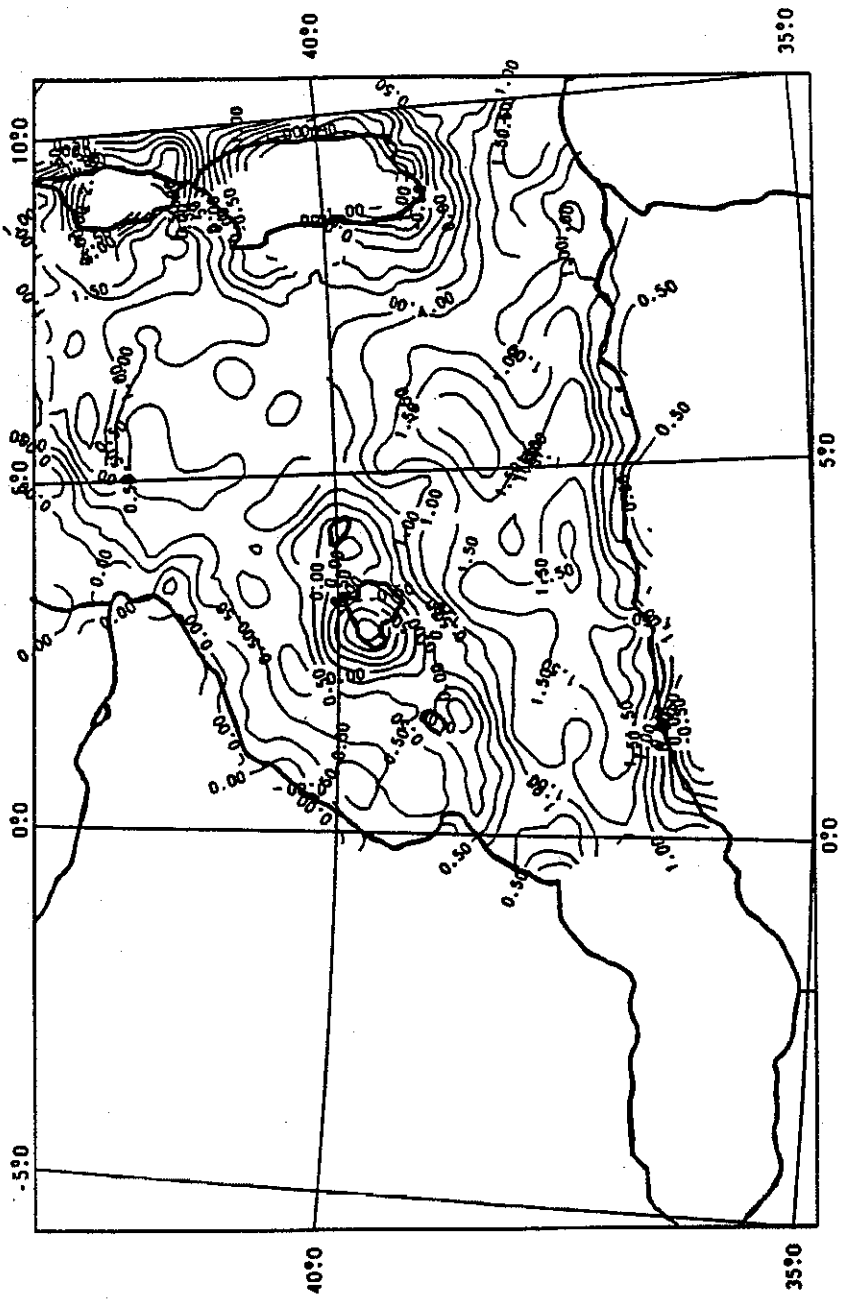
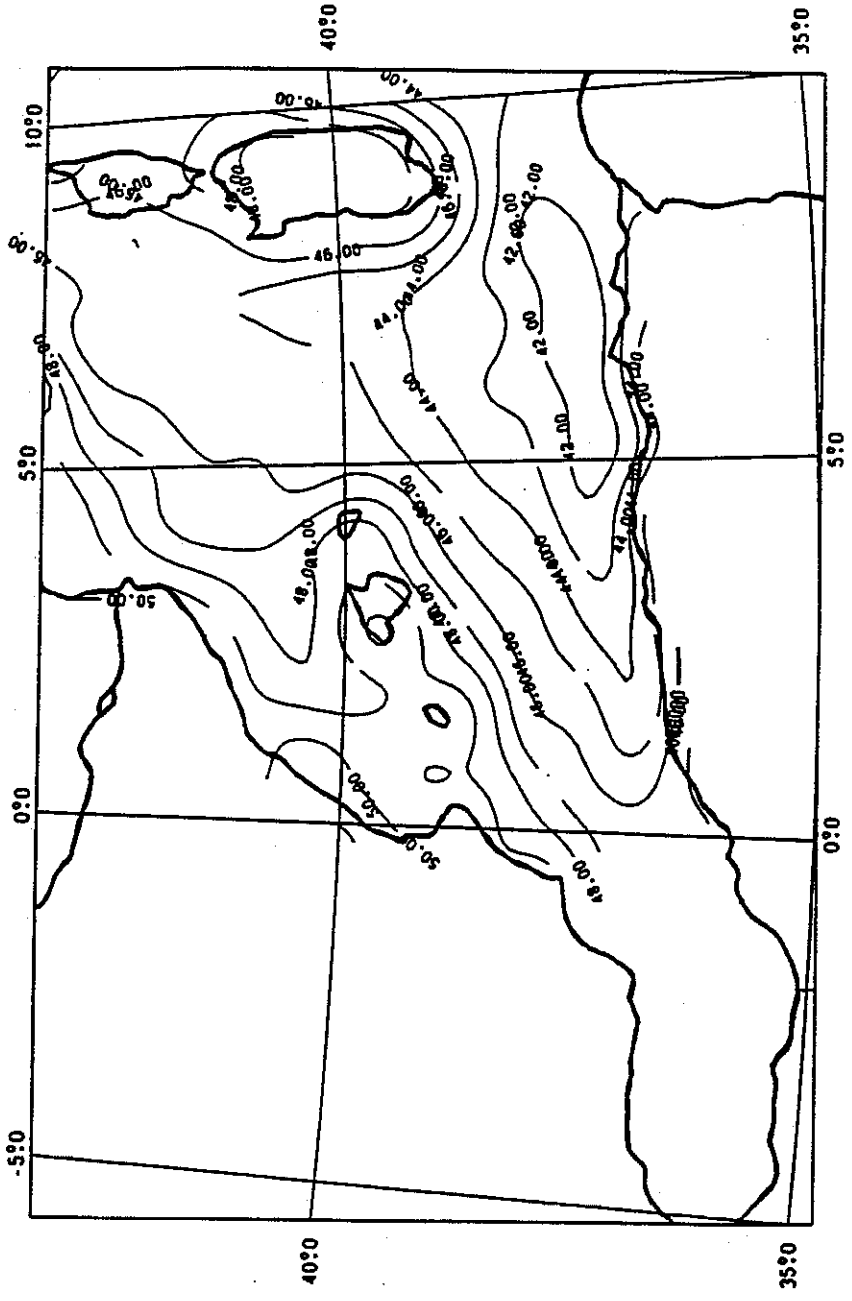
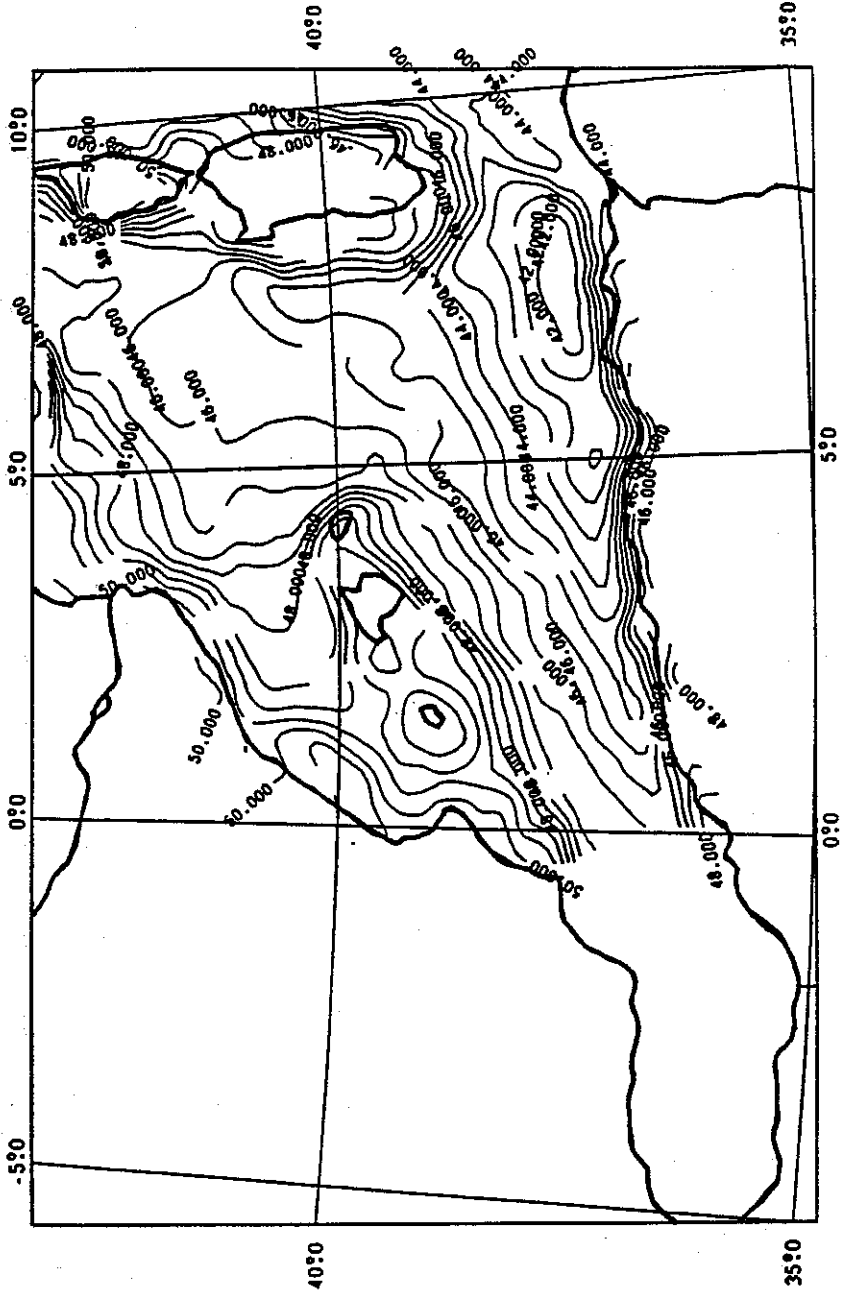
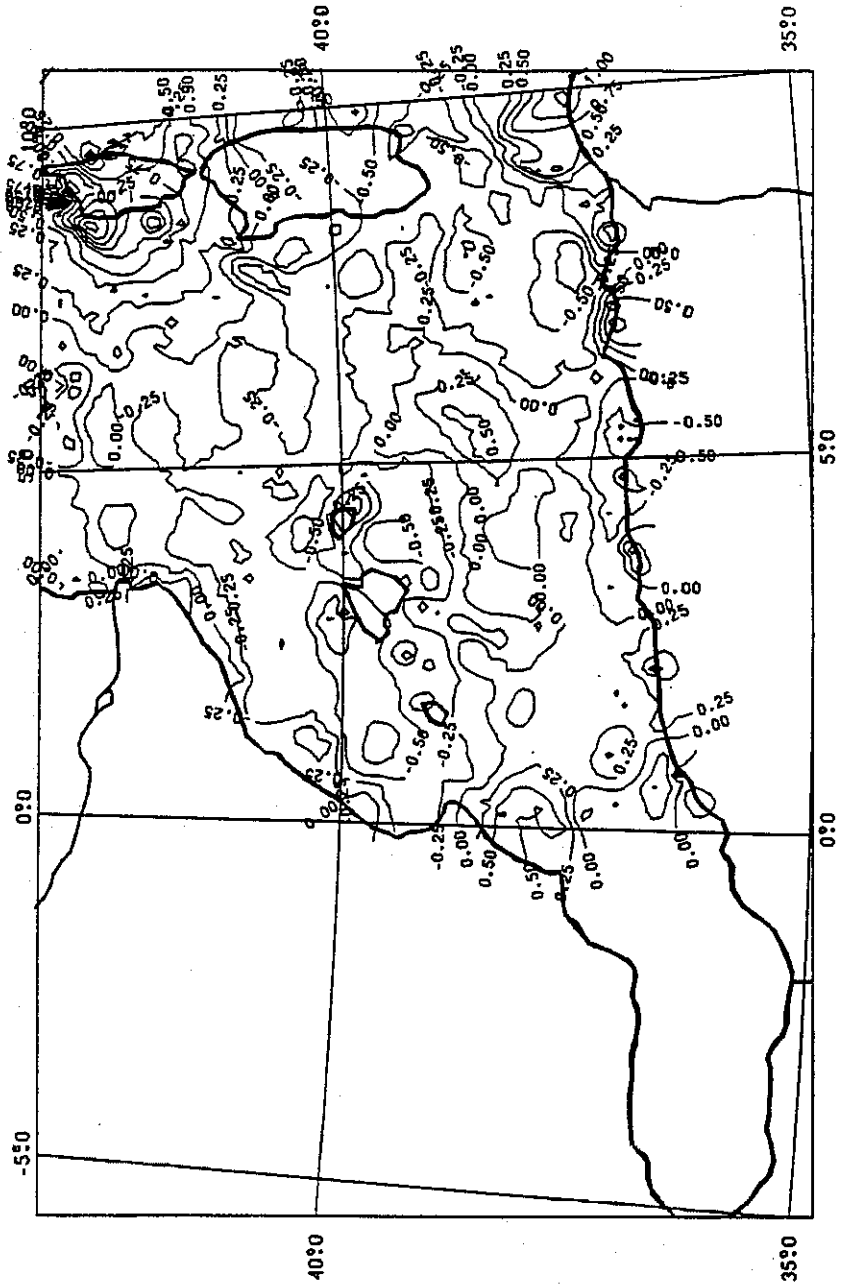


Fig. 8. - Stokes/FFT residual geoid (m)









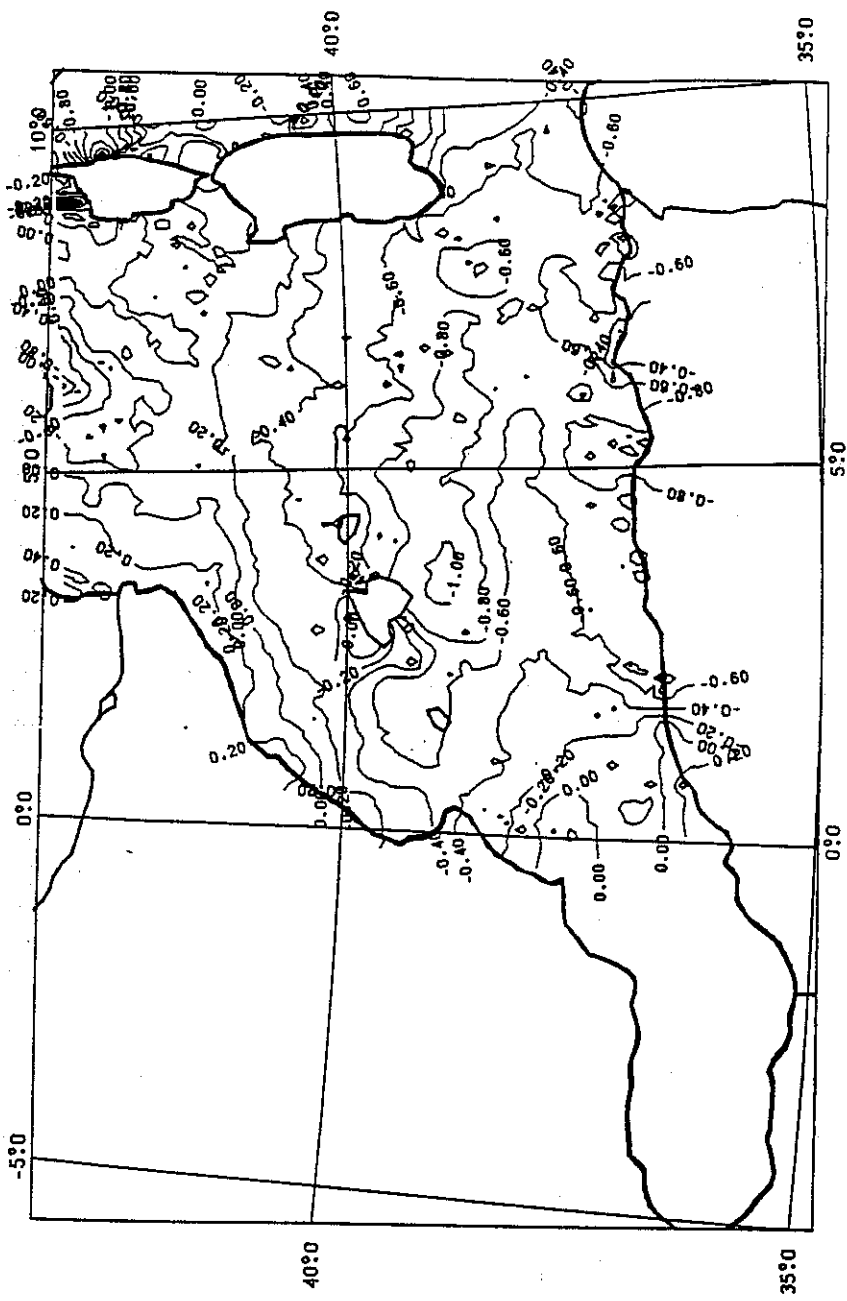


Fig. 14. - Sea Surface Topography (m)